International Journal of Nanoelectronics and Materials
IJNeaM
ISSN 1985-5761 | E-ISSN 2232-1535

Linear and nonlinear optical properties of rhodamine B, methylene blue, and saffron dyes in the presence of silver nanoparticles (Ag NPs)

Zena Karim[a] *, Raid Majeed Baiee[a], and Ghaleb Ali Al-Dahash[a]

[a]*Laser Physics Department, College of Science for Women, University of Babylon, Babylon, Iraq*
** Corresponding author: zina.mohammed.gsci199@student.uobabylon.edu.iq*

Received 11 May 2024, Revised 7 August 2024, Accepted 7 September 2024

ABSTRACT

In this study, we investigated the optical properties of the rhodamine B, methylene blue, and saffron dyes in the presented silver nanoparticles (Ag NPs). We detected that the absorption of the rhodamine B and methylene blue increased by interacting with NPs due to plasmon-induced quenching this effected can be utilized to manipulate and enhance optical properties and as a laser active medium. The highest value of the absorption coefficient for pure rhodium tincture was 222.86 cm^{-1}, and for saffron dye tinged with silver nanoparticles was 486.98 cm^{-1}. We studied the nonlinear optical responses of silver nanoparticles and these dyes. We detected that the silver nanoparticles have a high linear response at all selected laser excitations. In additionally, rhodamine B has a higher nonlinear response at a wavelength of 450 nm, which was further enhanced by the silver nanoparticles. Methylene blue has nonlinear responses, especially at the maximum absorption wavelength of 650 nm, and saffron dye showed nonlinear responses at all wavelengths, but the best response was at the 405 nm laser. The nanoparticles enhanced the nonlinear refraction of the saffron dye to fit the absorption spectra. The highest value of the nonlinear refractive index for saffron dye a doped with silver nanoparticles at a 405 nm laser was 3.48×10^{-11}. These results indicate that the addition of nanoparticles can enhance the nonlinear properties of these dyes with the use of dye-appropriate lasers in Z-Scan technology.

Keywords: Plasmonic nanoparticles, Rhodamine B dye, Z-Scan technique, Silver nanoparticles (Ag NPs), Negative refractive index

1. INTRODUCTION

The interaction between plasmonic nanoparticles and organic molecules have gained much research attention in recent times due to a large variety of applications like surface-enhanced Raman spectroscopy [1, 2] plasmon-enhanced fluorescence (3), nonlinear optical applications (4). Fast technological progress in optics has placed greater demand on the development of nonlinear optical materials (NLO) with prominent applications in optical limiting and all optical switching (4, 5). Nonlinear optics is the investigation of how intense light, like the laser, interacts with matter. Normally, only the laser light is adequately exceptional to alter the optical properties of a material. The optical reaction of a material typically scales straightly with the amplitude of the electric field, at high powers, however, the material properties can change more quickly. This leads to nonlinear effects consisting of self-focusing, saturated absorption (6, 7). Z-scan technique is the simplest and highest in sensitivity for computing nonlinear optical properties of materials (8, 9).

It also utilized to compute nonlinear refraction (NLR), nonlinear absorption (NLA) for solution, film models (10). The noble metal nanoparticles have immense applications primarily due to their property to generate substantially enhanced and highly localized electro-magnetic near-fields originating from localized surface plasmon resonances (11, 12). The high scale enhancement in the local electromagnetic field generated around metal objects and surfaces only when the sizes of the particles are much smaller than the irradiated wavelength (13). The inhomogeneities in the electromagnetic field have the potential to improve various light matter interactions in the sub wavelength regimes. The localized surface plasmon resonance (LSPR) originating from the collective oscillation of free electrons in resonance with the electromagnetic field of incident light could be tuned by controlling the size, composition, morphology, spatial arrangement and refractive index of the surrounding medium (14).

The fluorescence enhancement interactions of nanoparticles with organic molecules occur when the fluorescent molecules are placed in the vicinity of metal nano structures. The plasmonic-molecular resonance coupling interaction is also another type of interaction that exists between organic molecules and plasmonic nanoparticles, when the molecule has strong absorption in the LSPR of the nanoparticles. The refractive index dependent plasmon-organic molecule interaction in the neighborhood of plasmonic nanoparticle surface originates from the accumulation of induced polarization charges due to increased dielectric constant of the medium in the presence of organic molecule (15). The strengthening of electromagnetic intensities near plasmonic nanoparticle surface could also lead to enhancement in non-linear op tical responses like Raman scattering (16), that offer possibilities of novel non-linear nanoscale photonic

devices (17). Organic dyes are defined as hydrocarbon compounds, and organic dyes consist of large particles that have complex composition and have a wide absorbing and fluorescence spectrum in the visible spectrum areas because they contain chains and ultraviolet from the electromagnetic spectrum whose molecular weight is large because it contains chains composed of carbon atoms associated with separate bonds and others double (cheromophore) (18). Chrophor is characterized by light absorption in the ultraviolet and visual area, which makes the dye colored because the absorption transitions (s_0 - s_1) occurs in the visual area (19). Rhodamine B dye was used from the xanthine dye. It is in the form of solid green crystals or in the form of a reddish-violet powder. It has the ability to dissolve well in water and alcohol, and thus it will form a red fluorescent solution, and dilute solutions of this highly fluorescent substance, as well. This dye dissolves slightly in acids and bases, and it also dissolves in ethanol and gasoline (20). Methylene blue is known as methylthioninium chloride. It is used as a medicine and is also used as a dye. It is an industrial basic dye, with a dark green crystalline powder. It has a mild odor. Methylene blue is highly soluble in water, giving a blue color when dissolved in water. It is used as a dye in paper, silk, cosmetics, and laboratory procedures. Chemical and in human medical procedures. The compound can be used to treat methemoglobinemia (21, 22). Saffron contains more than 150 compounds (volatile and non-volatile). Saffron owes its sensory and functional properties mainly to the presence of its yellowish-red water-soluble carotenoid derivatives, which are synthesized throughout the flowering period but also during the entire production process (23). These compounds include crocin, crocetin (24).

2. EXPERIMENTAL PART

2.1. Materials

To prepare the dye solutions used rhodamine B, methylene blue, and saffron at a concentration of 1 x 10^{-3} M in the solvent used, water, and 0.0014 gm/ml of rhodamine b dye powder (B) and 0.0095 gm/ml of methylene blue dye powder were dissolved. and 0.01105gm/ml of saffron dye powder (in a volume of 30 ml of water). According to the following equation (1) (25),

$$W = \frac{C \times V \times M.W}{1000} \quad (1)$$

Figure 1 shows the prepared concentration of each dye.

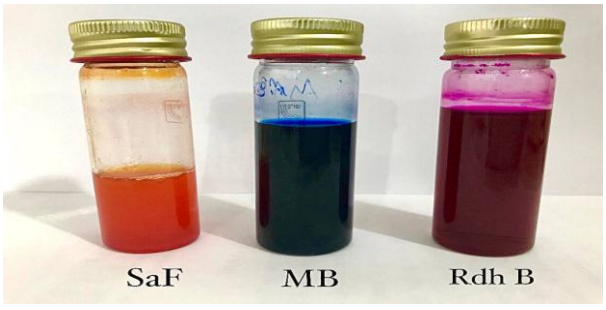

Figure 1. The prepared concentration of rhodamine B, methylene blue, and saffron dye.

2.2. Synthesis of Silver Nanoparticles (Ag NPs)

The process of laser ablation of Ag metal target (the silver plate ready, purity > 98%, purchased from CBI) was carried out in an aqueous medium using laser pulses(Q - switch Nd - YAG). Using a wavelength of 1064 nm, a repetition rate of 4 Hz, a pulse width of 5 ns, and a power of 700 mJ. The piece of Ag is placed at the bottom of a glass container, containing 6 ml of distilled water solution, and is bombarded with a laser with a number of 700 pulses, after which we obtain the formation of Ag NPs. As shown in Figure 2, the color of the solution changes into bright yellow confirming the formation of Ag NPs, the color of the solution changes to bright yellow confirming the formation of Ag NPs (see Figure 3).

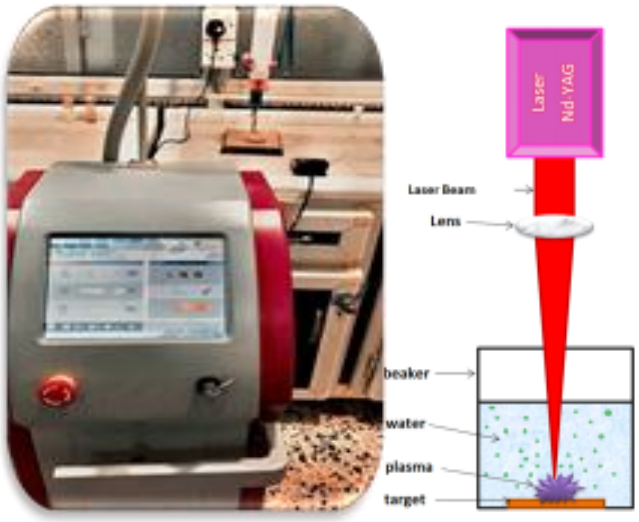

(a) (b)

Figure 2. Laser ablation system (a) Laser device used in pulsed laser ablation technology inside the advanced laboratory of the department of laser physics (b) Cross-section of the PLAL system.

Figure 3 Silver nanoparticles

2.3. Characterization Tools

A CECILCE CE 7200 (England) UV/ VIS/ NIR spectrophotometer has been used for UV-visible absorption studies, and a F96 Pro fluorescence emission spectrophotometer (England) has been utilized to record fluorescence emission measurements. The size and shape of the laser-synthesized Ag NPs were examined by the EM 208 transmission electron microscope (TEM).

2.4 Nonlinear Optical Analysis (Z-Scan)

The third-order nonlinear optical properties of natural dyes rhodamine B, methylene blue, and saffron with Ag NPs incorporated into them were studied using a z-scanning technique.

The laser light emitted through the sample is recorded as the samples are translated along the direction of propagation. Z-scan data were acquired using a semiconductor pumped solid-state laser. Lasers of different wavelengths (405 nm, 532 nm, 650 nm) were used and are characterized by high efficiency and stability.

A 1 mm thick quartz sample was translated through the propagation direction at a distance of approximately 60 mm either side of the focal point of the convex lens and the transmitted light intensity was recorded using a power detector. Both the transmitted and reference laser beam powers were recorded simultaneously and the ratio of the two was recorded using an optical laser beam power meter. The laser power was in the range of 12 to 70 mW, and a telephoto lens with a focal length of 8.5 cm was used. Figure 4 shows the Z-scan technology. Figure 5 shows the lasers used in this technology.

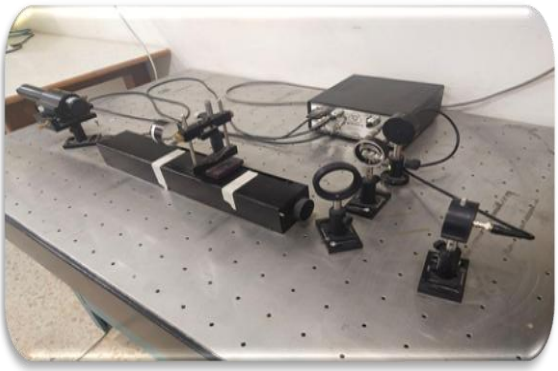

Figure 4 The Z-Scan technology arrangement

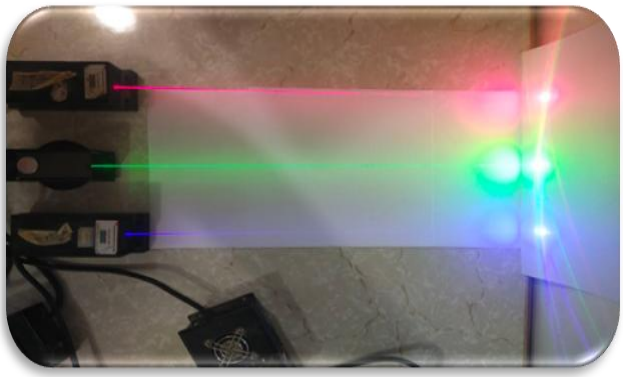

Figure 5 Lasers used in z-scanning technology

3. RESULTS AND DISCUSSION

3.1. Linear Optical Studies Absorption And Fluorescence Emission

3.1.1.Optical Characterization Of Silver Nanoparticle (Ag Nps)

Based on Figure 6, Ag NPs have an absorption spectrum in the visible spectrum region at the highest wavelength (419 nm) due to their possession of the phenomenon of surface plasmon resonance (SPR). Table 1 shows the absorption spectrum characteristics of Ag NPs.

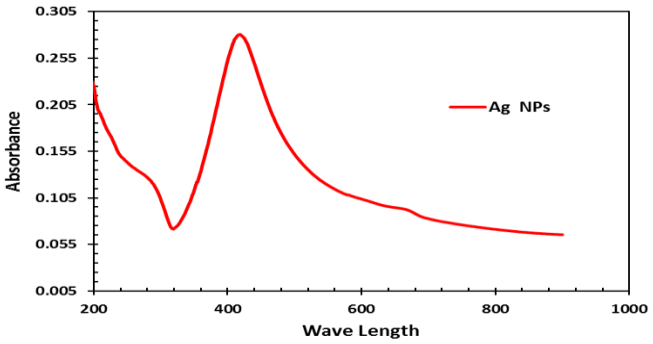

Figure 6. Optical absorption spectrum of Ag NPs.

Table 1 Absorption spectrum characteristics of Ag NPs

Absorption Peak Value	λ_{max} (nm)	$\alpha(cm^{-1})$
0.841449	419	64.595

Figure 7 shows TEM images of Ag NPs prepared using the pulsed laser spallation in liquids (PLAL) technique. It is noted from Figure 7 that the Ag NPs are spherical in shape. It is also noted from the statistical distribution of the nanosized size accompanying the TEM image, the average size of Ag NPs is about 13.58 nm.

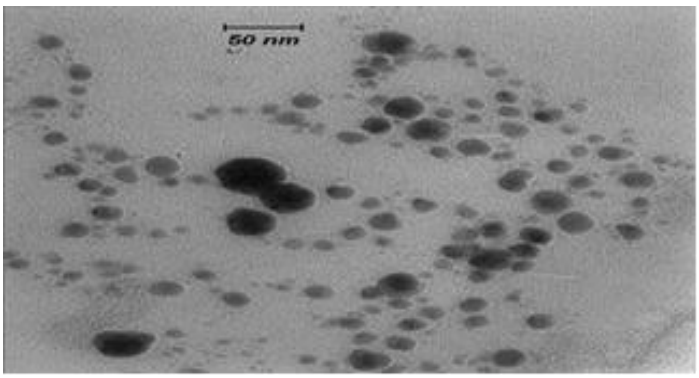

(a)

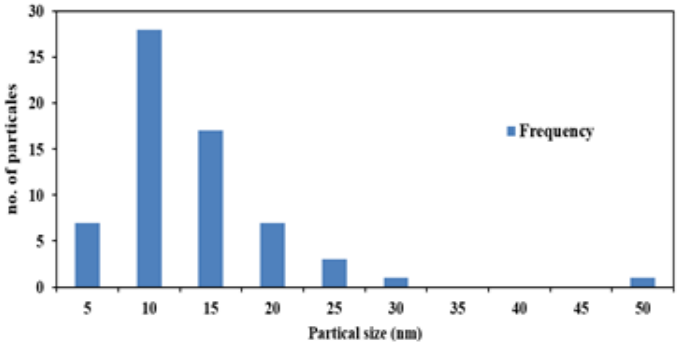

(b)

Figure 7. TEM images of silver nanoparticles (a) TEM image shows the shape and sizes of the Ag NPs (b) Statistical distribution of nanoparticle sizes.

3.1.2.Absorption And Fluorescence Emission Of Rhodamine B And Methylene Blue Laser Dyes After Mixing With Ag Nps

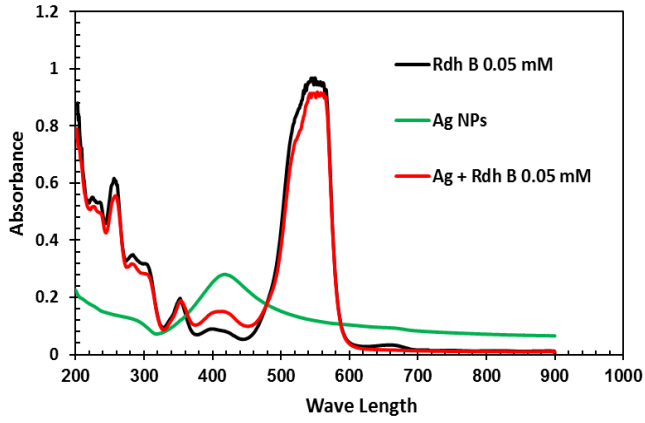

(a)

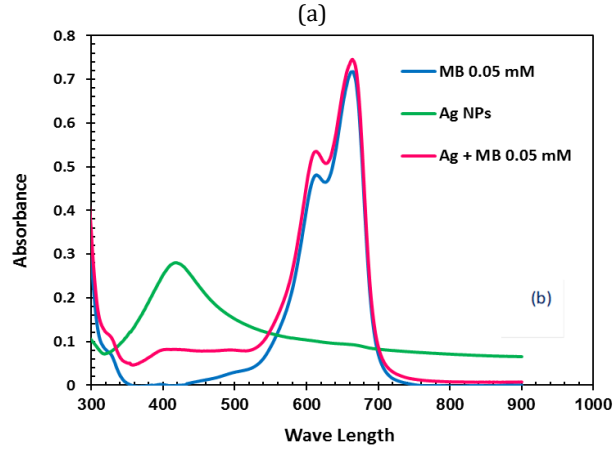

Figure 8. Optical absorption spectra (a) for rhodamine b when adding Ag NPs, (b) for methylene blue when adding Ag NPs.

Based on Figure 8, rhodamine B dye exhibits strong absorption in the 500-600 nm wavelength region, indicating π-π* transitions occurring in rhodamine B molecules, and that the presence of Ag NPs initially leads to an increase in the absorbance spectrum of the dye in the range 350-480 nm (the absorption region of the silver nanomaterial) and then a decrease in the intensity of the absorbance of the dye solution. This effect is attributed to the action of the plasmon present in silver nanoparticles influence electronic processes in dye molecules. Ag NPs enhance the local electromagnetic field and scatter light, leading to changes in the absorbance curve of the dye. At low concentrations, Ag NPs increase the intensity of scattered light and the number of excited molecules of the dye, resulting in increased absorbance, however, at higher concentrations, light scattering leads to a decrease in the absorbance intensity, and this result is consistent with the source (26). The main electronic transitions that contribute to the absorption spectrum of rhodamine B and methylene blue are the π-π* transitions. In Figure 8 (b), the spectrum of methylene blue shows strong absorption in the 600-700 nm wavelength region, indicating π-π* transitions occurring in methylene blue molecules. Adding Ag NPs to dyes like rhodamine B, methylene blue, and saffron can influence their electronic transitions, potentially involving both π-π* and n-π* transitions. Dyes like rhodamine B and saffron typically have negatively charged functional groups. Ag NPs, on the other hand, can have a positive surface charge due to adsorbed ions. This creates a columbic interaction, attracting electrons from the dye's highest occupied molecular orbital (HOMO) - which can be either a π or n orbital - towards the positively charged nanoparticle surface.

The columbic interaction can affect both π-π* and n-π* transitions in the dyes with the π-π* transitions if the HOMO involved in the transition is a π orbital, the interaction with the Ag NPs might slightly alter its energy level, potentially leading to a shift in the absorption peak (wavelength) associated with the π-π* transition.
n-π* transitions: similarly, if the HOMO is an n orbital (lone pair on a heteroatom), the Columbic interaction could influence its energy, potentially affecting the n-π* transition energy.

However, the exact nature of the shift (red or blue) it has been illustrated as discussed in Figure 8 and Figure 9. Table 2 shows the absorption spectrum characteristics of Ag NPs mixed with rhodamine B, methylene blue dye.

Table 2 Absorption spectra characteristics of rhodamine B and methylene blue dye solutions after adding Ag NPs represented by the highest absorbance intensity, maximum wavelength and absorption coefficient.

Dye	Absorption Peak Value	λ_{max} (nm)	$\alpha(cm^{-1})$
Rh B	2.903	549	222.860
Rh B + Ag NPs	2.756	553	211.642
MB	2.001	658	153.276
MB +Ag NPS	2.152	664	165.276

Rhodamine B dye dissolved in water showed a fluorescence emission with a peak value of 284.88 at the wavelength of 588.8 nm when excited with 553 nm light. Likewise, methylene blue dye dissolved in water showed a fluorescence emission with a peak value of 95.54 at the wavelength of 697 nm when excited with 664 nm light. It is

clear from Figure 9 that the fluorescent emission intensity of the dyes showed significant improvement when combined with Ag NPs as shown in Table 3. The interaction of dyes with Ag NPs results in improved fluorescence emission intensity due to enhanced light scattering, facilitating a greater interaction between the dyes and nanoparticles, as observed in Figure 9.

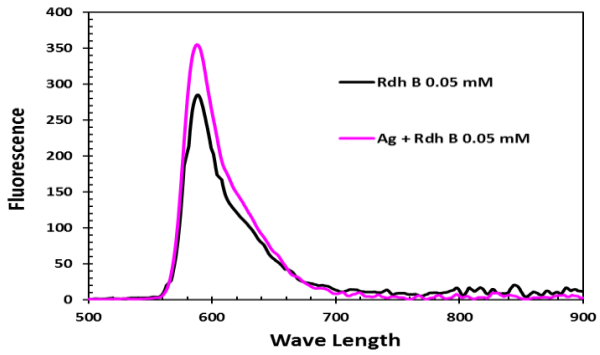

(a)

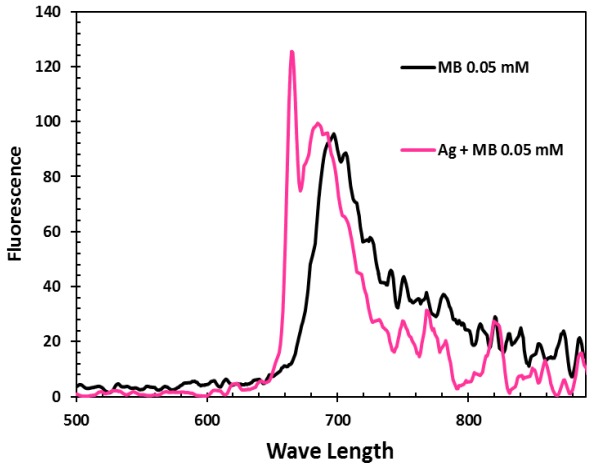

(b)

Figure 9. Fluorescence spectra of (a) Rhodamine dissolved in water before and after adding Ag NPs, (b) Methylene Blue dissolved in water before and after adding Ag NPs.

The increase in the fluorescence spectrum of the dye with the addition of nanoparticles can be explained by the phenomenon of fluorescence resonance energy transfer (FRET) (26). When the dye molecules are in close proximity to the nanoparticles, energy transfer occurs from the excited state of the dye to the nanoparticles, leading to enhanced fluorescence emission (27). This is because the nanoparticles act as efficient acceptors of the energy from the dye molecules, resulting in a higher fluorescence intensity (28). Additionally, the presence of nanoparticles can also lead to an increased local electromagnetic field, which further enhances the fluorescence emission of the dye (29). Therefore, the combination of the dye with silver nanoparticles results in an improved fluorescence spectrum due to the (FRET) process and the enhanced local electromagnetic field (30).

Table 3 Emission spectrum characteristics of rhodamine B and methylene blue dye dissolved in water before and after adding Ag NPs.

Dye	λ_{max} (nm)	Fluorescence
rhodamine B	584	284.88
rhodamine B + Ag NPs	587.8	355.02
methylene blue	697	95.54
methylene blue +Ag NPS	664.7	147.91

3.1.3. Absorption Of Natural Saffron Dye Before and After The Addition Of Silver Nanoparticles (Ag Nps)

The effect of adding Ag NPs on the absorption spectra of the concentration of saffron dye dissolved in water was studied. Figure 10 shows the UV spectra of colloidal Ag NPs mixed with the natural saffron dye.

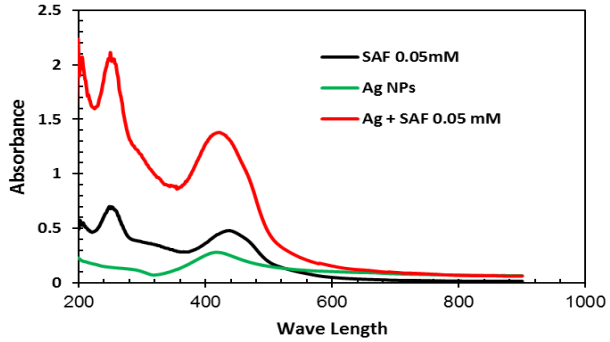

Figure 10. Optical absorption spectrum of saffron dye after addition of Ag NPs

The absorption spectrum of saffron dye between 300 and 500 nm results from a combination of π-π* and n-π* transitions. The addition of Ag NPs to the saffron dye solution resulted in an increase in the absorption spectrum of the dye. This increase in absorption can be attributed to the interaction between the saffron dye molecules and the Ag NPs. The presence of the Ag NPs alters the optical properties of the dye, leading to enhanced absorption of light at specific wavelengths (26). The exact mechanism behind this phenomenon may involve the plasmonic properties of the Ag NPs, which can enhance the local electromagnetic field and promote the absorption of light by the dye molecules (31). Table 4 shows characteristics of absorption spectra of Ag NPs mixed with saffron dye.

Table 4 characteristics of absorption spectra of Ag NPs mixed with saffron dye

dye	Absorption Peak Value	λ_{max} (nm)	$\alpha(cm^{-1})$
saffron	2.096	249	160.97
Saffron+ Ag NPs	2.112	250	486.98

3.2. Nonlinear Optical Analysis

3.2.1 Nonlinear Optical Analysis Of Ag Nps

The results showed that Ag NPs have a negative nonlinear refractive index, that is, n_2 is a negative value, and the nonlinear permeability curves also appear with a peak and then a bottom. It is obvious from Figure 11 that Ag NPs have higher negative refractive index at 405 nm wavelength. This could be attributed to the distinct surface plasmon absorption peak corresponding to Ag NPs at 419 nm. On the other hand, Ag NPs have less negative refractive index at 650 nm and 532 nm. The nonlinear refractive index values of the Ag NPs are listed in Table 5.

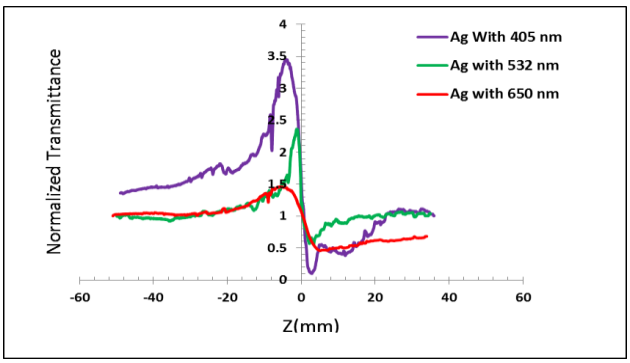

Figure 11. Nonlinear refraction of Ag NPs with effect of three wavelengths (405 nm, 532 nm, 650 nm).

Table 5 Nonlinear properties of Ag NPs prepared by the method of laser ablation in water under the influence of several wavelengths

λ(nm)	P (mW)	I_0(MW/m^2)	L_{eff}(m)	ΔT	n_2 (m2/W)
405	2.01	13.557	0.000970	3.356757	$4.18*10^{-11}$
532	40	22.643	0.000985 5	1.804734	$1.85*10^{-11}$
650	59.55	58.33	0.000989	1.005979	$4.47*10^{-12}$

It is clear from the data in Table 5 that the largest absolute value of the nonlinear refractive index is located at 405 nm because the wavelength (405 nm) is within the peak of the absorption band of Ag NPs. The value of the nonlinear refractive index begins to decrease with increasing wavelength due to the decrease in linear absorption. Due to the SPR of Ag NPs, the light energy is efficiently absorbed and then transferred to the water via non-radiative relaxation processes (32). This increases the local temperature in the water and the thermal gradient leads to a change in the local refractive index because the local refractive index decreases with increasing temperature. For most liquids such as water. The large values of the nonlinear refractive index at short wavelength can be attributed to the high energy of these photons compared to other wavelengths. Higher energy photons can excite samples to higher energy levels. This means more non-radiative relaxations and hence higher temperature, leading to higher associated nonlinearities (33).

3.2.1 Nnri Of Dyes (Rdh B, Mb, Saf) Before And After Adding Ag Nps Under The Influence Of Different Wavelengths

The nonlinear refractive index (NNRI) of rhodamine B, methylene blue, and saffron dyes was studied before and after adding Ag NPs under the influence of different wavelengths (405, 532, 650 nm). Figures 12, 13 and 14 show the closed aperture curves for all dyes before and after adding Ag NPs, and they have negative refractive indices under the influence of the wavelengths used.

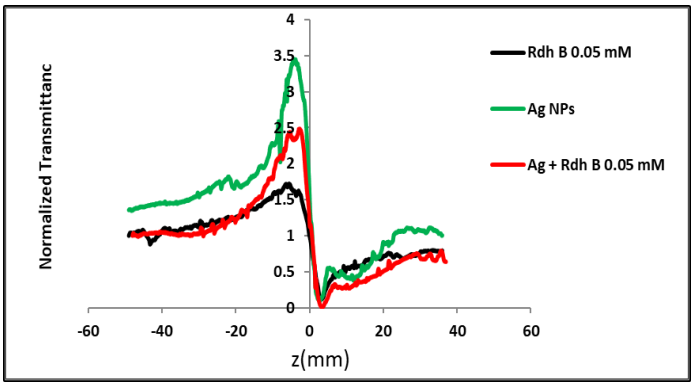

(a)

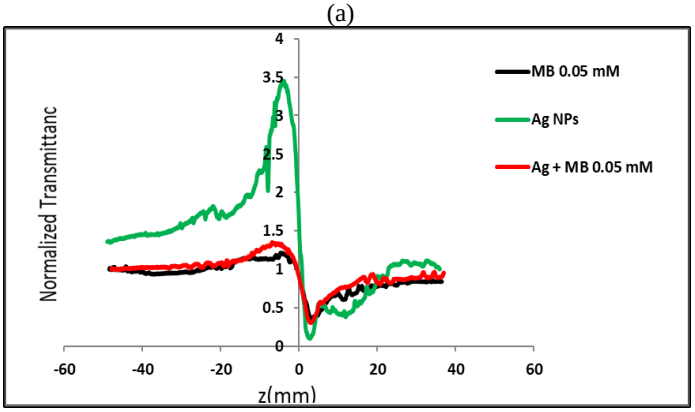

(b)

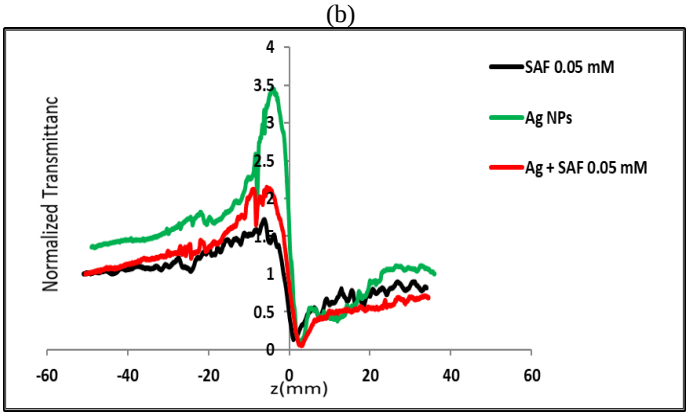

(c)

Figure 12. Nonlinear transmittance of rhodamine B, methylene blue, and saffron dyes before and after adding Ag NPs at 405 nm (a) rhodamine B (b) methylene blue (c) saffron.

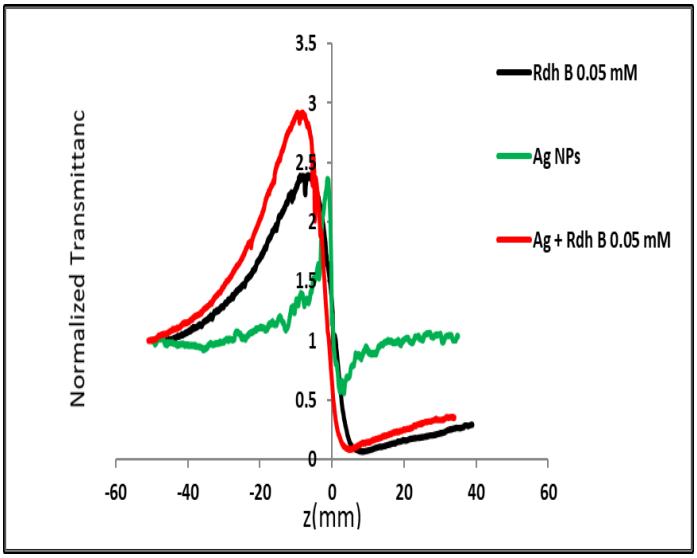

(a)

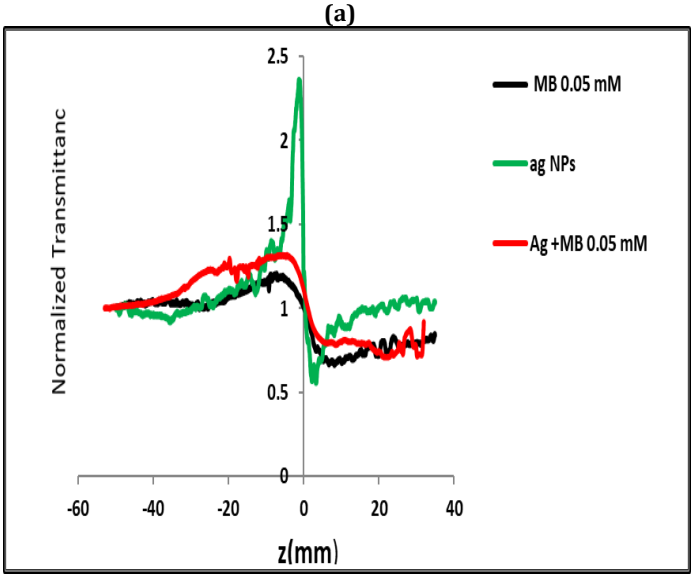

(b)

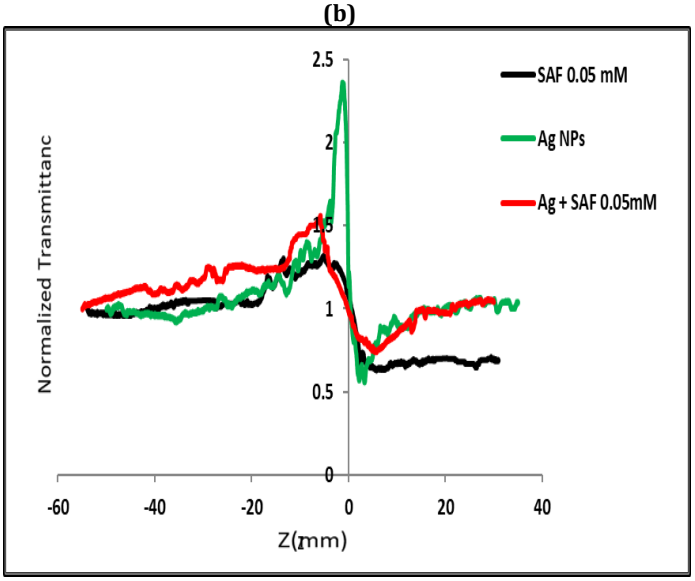

(c)

Figure 13. Nonlinear transmittance of rhodamine B, methylene blue, and saffron dyes before and after adding Ag NPs at 532 nm (a) rhodamine B (b) methylene blue (c) saffron.

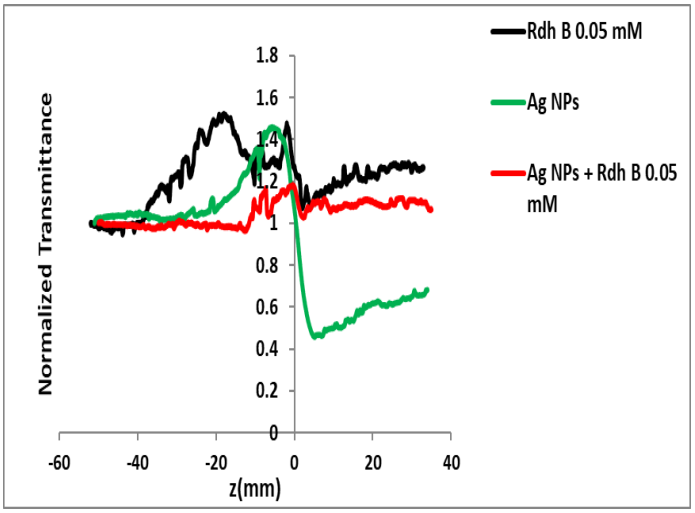

(a)

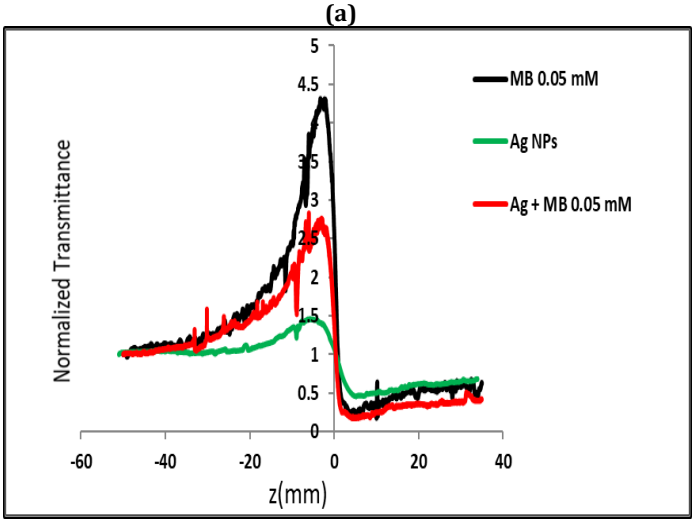

(b)

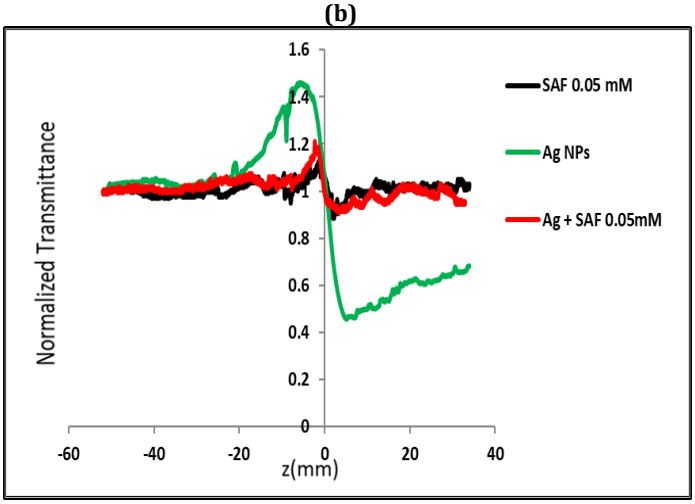

(c)

Figure 14. Nonlinear transmittance of rhodamine B, methylene blue, and saffron dyes before and after adding Ag NPs at and 650 nm. (a) rhodamine B (b) methylene blue (c) saffron.

Figure 12 and 13 show the nonlinear transmittance of rhodamine B, methylene blue, and saffron dye before and after adding Ag NPs under the influence of two lasers with wavelengths of 405 and 532 nm. The NNRI of all dyes was increased by adding Ag NPs to each dye under the influence of wavelength 405 and 532 nm, because both laser wavelengths (405 and 532 nm) fall within the

absorption spectrum range of Ag NPs. This increased the NNRI of all the dyes by transferring heat

Table 6 Nonlinear properties of rhodamine B dye after adding Ag NPs under the influence of different wave lengths.

rhodamine B					
λ(nm)	C (mM)	I_0(MW/m²)	L_{eff}(m)	ΔT	n_2 (m2/W)
405	0.05 Rdh	91.056	0.00098994	1.60559	2.92*10^{-12}
405	0.05 Rdh B +Ag NPs	91.056	0.00098296	2.479865	4.54*10^{-12}
532	0.05 Rdh	17.751	0.00090251	2.332386	3.10*10^{-11}
532	0.05 Rdh	17.751	0.0009112	2.842105	3.74*10^{-11}
650	0.05 Rdh	58.331	0.000996	0.57916	2.55*10^{-12}
650	0.05 Rdh	58.331	0.000998	0.2215	9.75*10^{-13}

Table 7 Nonlinear properties of methylene blue dye after adding Ag NPs under the influence of different wave lengths.

methylene blue					
λ(nm)	C (mM)	I_0(MW/m²)	L_{eff}(m)	ΔT	n_2 (m2/W)
405	0.05 MB	89.707	0.000997	0.877841	1.61*10^{-12}
405	0.05 MB +Ag NPs	89.707	0.000991	1.052083	1.94*10^{-12}
532	0.05 MB	13.585	0.000984	0.54494	8.67*10^{-12}
532	0.05 MB +Ag NPs	13.585	0.000989	0.61149	9.68*10^{-12}
650	0.05 MB	39.181	0.000901	4.13901	3*10^{-11}
650	0.05 MB + Ag NPs	39.181	0.000927	2.65094	1.87*10^{-11}

from the Ag NPs to the dye solution where the thermal kerr effect appeared. Light energy is efficiently absorbed and then transferred to water via non-radiative relaxation processes. This increases the local temperature in the water. The temperature gradient leads to a change in the local refractive index because the local refractive index decreases with increasing temperature for most liquids such as water. By observing the results in figure 14 , we find that the nonlinear refractive index values of all the dyes decrease when Ag NPs are added to them under the influence of the wavelength of 650 nm. This is because the laser wavelength (650 nm) lies outside the absorption spectrum of Ag NPs. This resulted in a decrease in the nonlinear refractive index value of each pigment under the influence of the wavelength of 650 nm. The large values of the nonlinear refractive index at short wavelength can be attributed to the high energy of these photons compared to other wavelengths. Higher energy photons can excite samples to higher energy levels. This means more non-radiative relaxation processes and hence higher temperature, leading to higher associated nonlinearities (34,35). The nonlinear refractive index values for each dye were calculated before and after adding nanoparticles under the influence of different wavelengths and listed in Tables 6 , 7 and 8 below.

Table 8 Nonlinear properties of saffron dye after adding Ag NPs under the influence of different wave lengths.

Saffron					
λ(nm)	C (mM)	I_0(MW/m²)	L_{eff}(m)	ΔT	n_2 (m²/W)
405	0.05 SAF	18.548	0.0009572	1.59195	1.47*10^{-11}
405	0.05 SAF	16.862	0.0009369	3.35676	3.48*10^{-11}
532	0.05 SAF	39.689	0.00098609	0.69298	1.23*10^{-11}
532	0.05 SAF	11.853	0.00098588	0.820873	1.50*10^{-11}
650	0.05 SAF	42.12	0.000996	0.241206	1.47*10^{-12}
650	0.05 SAF +	42.12	0.000994	0.232597	1.42*10^{-12}

CONCLUSIONS

The structural properties of Ag NPs were studied, and it was found that they have a spherical shape and an average size of about 13.58 nm. It was also noted that silver nanoparticles (Ag NPs) have an absorption spectrum in the visible spectrum region at the highest wavelength of 419 nm because they possess the phenomenon of surface plasmon resonance (SPR). The behavior of rhodamine B, methylene blue and saffron was studied in terms of linear optical properties and nonlinear optical responses.

The dyes showed specific absorption peaks, and the addition of NPs also affected the characteristics of the absorption spectra of the rhodamine B and MB dyes. The reason for this increase is due to a phenomenon called “plasma-induced quenching.” This phenomenon occurs due to various processes such as energy transfer, or electron transfer. Addition of Ag NPs to the saffron dye solution increased the absorption spectrum of the dye, The highest value of the absorption coefficient for pure rhodium tincture was 222.86 cm^{-1}, and for saffron dye tinged with Ag NPs was 486.98 cm^{-1}. This increase in absorption can be attributed to the interaction between saffron dye molecules and Ag NPs. The Ag NPs also affected the characteristics of the fluorescence spectrum of Rdh B and MB dyes. The increase in the fluorescence spectrum of the dyes with the addition of nanoparticles can be explained through the phenomenon of fluorescence resonance

energy transfer. Rhodamine B dye showed the highest nonlinear response at 405 nm excitation wavelength, and Ag NPs enhanced their response at the same wavelength. Likewise, methylene blue and saffron dye showed significant nonlinear responses, especially at the maximum dye absorption wavelength, which was further enhanced by Ag NPs, as the best nonlinear response of the dyes was after the addition of Ag NPs under the influence of a 405 nm laser because it falls within the spectrum absorption of Ag NPs ,The highest value of the nonlinear refractive index for saffron dye a doped with Ag NPs at a 405 nm laser was 3.48×10^{-11}.

The results of this study indicate that the addition of nanoparticles can enhance the nonlinear properties of these dyes, as the thermal Kerr effect appeared in all samples studied, which leads to improvement in applications that require optical behavior, such as optical power limiters, sensors and improving solar cells. The improvement also led to the improvement of the linear and nonlinear properties. Linearization of dyes by adding Ag NPs to their use as an active laser medium in random lasers.

REFERENCES

[1] Y. Fang, N.-H. Seong, and D. D. Dlott, "Measurement of the Distribution of Site Enhancements in Surface-Enhanced Raman Scattering," Science, vol. 321, no. 5887, pp. 388–392, 2008, doi: https://doi.org/10.1126/science.1159499.

[2] D.-K. Lim, K.-S. Jeon, H. M. Kim, J.-M. Nam, and Y. D. Suh, "Nanogap-engineerable Raman-active nanodumbbells for single-molecule detection," Nature Materials, vol. 9, no. 1, pp. 60–67, 2010, doi: https://doi.org/10.1038/nmat2596.

[3] A. Kinkhabwala, Z. Yu, S. Fan, Y. Avlasevich, K. Müllen, and W. E. Moerner, "Large single-molecule fluorescence enhancements produced by a bowtie nanoantenna," Nature Photonics, vol. 3, no. 11, pp. 654–657, 2009, doi: https://doi.org/10.1038/nphoton.2009.187.

[4] R. R. Krishnamurthy and R. Alkondan, "Nonlinear characterization of Mercurochrome dye for potential application in optical limiting," Optica Applicata, vol. 40, no. 1, pp. 187–196, 2010.

[5] N. Venkatram, D. Narayana Rao, L. Giribabu, and S. Venugopal Rao, "Femtosecond nonlinear optical properties of alkoxy phthalocyanines at 800nm studied using Z-Scan technique," Chemical Physics Letters, vol. 464, no. 4, pp. 211–215, 2008, doi: https://doi.org/10.1016/j.cplett.2008.09.029.

[6] R. W. Boyd, A. L. Gaeta, and E. Giese, "Nonlinear Optics," in Springer Handbook of Atomic, Molecular, and Optical Physics, G. W. F. Drake, Ed., Cham: Springer International Publishing, 2023, pp. 1097–1110. doi: 10.1007/978-3-030-73893-8_76.

[7] F. Träger, Springer handbook of lasers and optics, vol. 2. Springer, 2012.

[8] Q. Mohammed Ali and P. K. Palanisamy, "Investigation of nonlinear optical properties of organic dye by Z-scan technique using He–Ne laser," Optik, vol. 116, no. 11, pp. 515–520, 2005, doi: https://doi.org/10.1016/j.ijleo.2005.05.001.

[9] A. Y. Nooraldeen, A. N. Dhinaa, and P. K. Palanisamy, "Nonlinear Optical Properties of Acid Orange 10 Dye By Z-Scan Technique Using Ar+ Laser," J. Nonlinear Optic. Phys. Mat., vol. 16, no. 03, pp. 359–366, 2007, doi: https://doi.org/10.1142/S0218863507003743.

[10] S. Qi et al., "Effective indexes of refraction and limiting properties of ethyl red," Optik, vol. 118, no. 9, pp. 425–429, 2007, doi: https://doi.org/10.1016/j.ijleo.2006.03.029.

[11] D. M. AL-Aqmar, Z. H. El Gohary, H. A. Othman, and M. T. H. Abou Kana, "Optical characterization of Coumarin 334 hybrid with silver nanoparticles in imidazolium-based ionic liquid," Dyes and Pigments, vol. 165, pp. 361–371, 2019, doi: https://doi.org/10.1016/j.dyepig.2019.01.046.

[12] V. Dave, R. Sharma, C. Gupta, and S. Sur, "Folic acid modified gold nanoparticle for targeted delivery of Sorafenib tosylate towards the treatment of diabetic retinopathy," Colloids and Surfaces B: Biointerfaces, vol. 194, p. 111151, Oct. 2020, doi: https://doi.org/10.1016/j.colsurfb.2020.111151.

[13] S. Lal, S. Link, and N. J. Halas, "Nano-optics from sensing to waveguiding," Nature Photonics, vol. 1, no. 11, pp. 641–648, 2007, doi: https://doi.org/10.1038/nphoton.2007.223.

[14] M.-H. Tseng, C.-C. Hu, and T.-C. Chiu, "A fluorescence turn-on probe for sensing thiodicarb using rhodamine B functionalized gold nanoparticles," Dyes and Pigments, vol. 171, p. 107674, 2019, doi: https://doi.org/10.1016/j.dyepig.2019.107674.

[15] H. Chen et al., "Plasmon–molecule interactions," Nano Today, vol. 5, no. 5, pp. 494–505, 2010, doi: https://doi.org/10.1016/j.nantod.2010.08.009.

[16] J. Zhang, Y. Fu, M. H. Chowdhury, and J. R. Lakowicz, "Metal-Enhanced Single-Molecule Fluorescence on Silver Particle Monomer and Dimer: Coupling Effect between Metal Particles," Nano Lett., vol. 7, no. 7, pp. 2101–2107, 2007, doi: https://doi.org/10.1021/nl071084d.

[17] M. I. Stockman, D. J. Bergman, C. Anceau, S. Brasselet, and J. Zyss, "Enhanced Second-Harmonic Generation by Metal Surfaces with Nanoscale Roughness: Nanoscale Dephasing, Depolarization, and Correlations," Phys. Rev. Lett., vol. 92, no. 5, p. 057402, 2004, doi: https://doi.org/10.1103/PhysRevLett.92.057402.

[18] W. Demtröder, "Laser spectroscopy: Basic concepts and instrumentation," NASA STI/Recon Technical Report A, vol. 82, p. 12273, 1981.

[19] F. P. Schäfer, "Dye lasers and laser dyes in physical chemistry," in Dye Lasers: 25 Years, M. Stuke, Ed., Berlin, Heidelberg: Springer Berlin Heidelberg, 1992, pp. 19–36. doi: 10.1007/3-540-54953-6_2.

[20] F. P. Schäfer, "1. Principles of dye laser operation," in Dye Lasers, vol. 1, F. P. Schäfer, Ed., Berlin, Heidelberg: Springer Berlin Heidelberg, 1990, pp. 1–89. doi: 10.1007/3-540-51558-5_7.

[21] V. V. Tkach et al., "The Theoretical Description For Methylene Blue Electrochemical Determination And

Decolorization, Assisted By Polynaphthoquinones/Ti/Tio2/Vo(Oh) Composite," Applied Journal of Environmental Engineering Science, vol. 6, no. 1, Art. no. 1, 2020, doi: https://doi.org/10.48422/IMIST.PRSM/ajees-v6i1.15866.

[22] J. I. Clifton and J. B. Leikin, "Methylene Blue," American Journal of Therapeutics, vol. 10, no. 4, pp. 289–291, 2003.

[23] R. Armellini et al., "In vitro starch digestibility and fate of crocins in pasta enriched with saffron extract," Food Chemistry, vol. 283, pp. 155–163, 2019, doi: https://doi.org/10.1016/j.foodchem.2019.01.041.

[24] A. Gani, R. Jan, B. A. Ashwar, Z. ul Ashraf, A. Shah, and A. Gani, "Encapsulation of saffron and sea buckthorn bioactives: Its utilization for development of low glycemic baked product for growing diabetic population of the world," LWT, vol. 142, p. 111035, 2021, doi: https://doi.org/10.1016/j.lwt.2021.111035.

[25] A. K. Aimukhanov, N. Kh. Ibrayev, A. A. Ishchenko, and A. V. Kulinich, "Effect of Silver and Gold Nanoparticles on the Spectral and Luminescent Properties of a Merocyanine Dye," Theoretical and Experimental Chemistry, vol. 54, no. 6, pp. 369–374, 2019, doi: https://doi.org/10.1007/s11237-019-09583-9.

[26] P. Chandulal Vithalani and N. Sumantray Bhatt, "Solar Light Assisted Degradation of Rhodamine B Dye by Chemically Synthesized Silver Nanoparticles," The holistic approach to environment, vol. 13, no. 3, pp. 83–91, 2023, doi: https://doi.org/10.33765/thate.13.3.1.

[27] suci wulandari, A. N. Rahma, S. Wahyuni, and B. Lubis, "Analiysis of Rhodamine B Dyestuffs on Liptint Using Uv-Vis Spectrophotometry Method," JFM, vol. 5, no. 2, pp. 184–191, 2023, doi: https://doi.org/10.35451/jfm.v5i2.1295.

[28] S. Sulastri, R. Riani, and S. Farikha, "Review Artikel: Analisis Kandungan Rhodamin B Dalam Makanan Dan Minuman," COMSERVA: Jurnal Penelitian dan Pengabdian Masyarakat, vol. 2, no. 10, pp. 2429–2435, 2023, doi: https://doi.org/10.59141/comserva.v2i10.701.

[29] Yusser R.Mohammed and Waleed S.Abdull wahab, "Studying The Fluorescence Resonance Energy Transfer between Fluorescein and Rhodamine B in an aqueous solution," cbej, vol. 28, no. 117, pp. 1–12, 2022, doi: https://doi.org/10.35950/cbej.v28i117.9066.

[30] J. Sharma, S. Sharma, U. Bhatt, and V. Soni, "Toxic effects of Rhodamine B on antioxidant system and photosynthesis of Hydrilla verticillata," Journal of Hazardous Materials Letters, vol. 3, p. 100069, 2022, doi: https://doi.org/10.1016/j.hazl.2022.100069.

[31] G. Sun, J. Huang, S. Hao, and Q. Zhang, "Electroless plating silver nanoparticles mixed in oxidized microcrystalline cellulose for microwave absorption applications," Cellulose, vol. 30, no. 9, pp. 5761–5775, 2023, doi: https://doi.org/10.1007/s10570-023-05241-5.

[32] R. González-Campuzano et al., "Saturable absorption and negative nonlinear refraction index evolution in silver nanoparticles colloids," Optics & Laser Technology, vol. 159, p. 108989, 2023, doi: https://doi.org/10.1016/j.optlastec.2022.108989.

[33] T. Mohamed et al., "Excitation Wavelength and Colloids Concentration-Dependent Nonlinear Optical Properties of Silver Nanoparticles Synthesized by Laser Ablation," Materials, vol. 15, no. 20, 2022, doi: https://doi.org/10.3390/ma15207348.

[34] N. Shokoufi and S. Nouri Hajibaba, "The third-order nonlinear optical properties of gold nanoparticles-methylene blue conjugation," Optics & Laser Technology, vol. 112, pp. 198–206, 2019, doi: https://doi.org/10.1016/j.optlastec.2018.09.058.

[35] U. M. Parvin and M. B. Ahamed, "Nonlinear optical properties of methyl blue dye by Z-scan technique," Optik, vol. 126, no. 5, pp. 551–553, 2015, doi: https://doi.org/10.1016/j.ijleo.2015.01.001.